Angular distribution of photons for the simultaneous excitation and ionization of He-like uranium ions in relativistic ion-atom collisions

S. Salem[*]

Institut für Kernphysik, Universität Frankfurt, D-60438 Frankfurt, Germany,
GSI Helmholtzzentrum für Schwerionenforschung, D-64291 Darmstadt, Germany, and
Department of Physics, Al-Balqa' Applied University, 19117 Al-Salt, Jordan

Th. Stöhlker

GSI Helmholtzzentrum für Schwerionenforschung, D-64291 Darmstadt, Germany,
Helmholtz-Institut Jena, D-07743 Jena, Germany, and
Physikalisches Institut, Ruprecht-Karls-Universitaet Heidelberg, D-69120 Heidelberg, Germany

A. Bräuning-Demian, S. Hagmann, C. Kozhuharov, and D. Liesen

GSI Helmholtzzentrum für Schwerionenforschung, D-64291 Darmstadt, Germany

A. Gumberidze

ExtreMe Matter Institute EMMI and Research Division, GSI Helmholtzzentrum für Schwerionenforschung, D-64291 Darmstadt, Germany

Simultaneous ionization and excitation processes are studied for initially He-like uranium ions in collisions with xenon gaseous targets at relativistic energy, 220 MeV/u. The virtue of investigating the process of simultaneous excitation and ionization is that one electron ends up in the continuum, while the other electron ends up in a hydrogen-like final state. Experimentally, this process can be identified by observing the radiative decay of the excited levels in coincidence with ions that lost one electron (U^{91+}). In particular, owing to the large fine-structure splitting of H-like U, the angular distribution of photons for the simultaneous ionization and excitation into the different total angular momentum $j = 1/2$ and $j = 3/2$ states of the L shell is determined directly from the observed yields of $Ly_{\alpha 1}$ and $Ly_{\alpha 2}$ radiation at various observation angles. The experimental data show a progress for the dependence of the alignment on the collision impact parameter. It is shown that the current results confirm the theoretical predictions based on the independent-particle approximation and first-order perturbation, for which the simultaneous ionization and excitation processes occur at small impact parameter.

I. INTRODUCTION

During ion-atom collisions, the excitation and/or the ionization of bound electrons of the collision partners can occur and also electrons can be transferred from one collision partner to the other. For the relativistic atomic collisions, the basic processes have been studied in great detail during the last decades in different collision systems [1,2]. Of considerable interest are still the single-electron processes in atomic collisions. These effects are produced by a significant mutual interaction of two electrons whose theoretical description requires an extension of the independent-electron model. The understanding of these phenomena requires an understanding of the many-body problem encountered in atomic collisions. Single-electron processes have been studied, both experimentally and theoretically, mainly for nonrelativistic systems [3,4]. Most previous experiments have focused on two-electron processes in helium, since this is the simplest system containing more than one electron [5]. Total cross sections of multiple processes for a two-electron system in collisions with neutral targets at low velocities have been studied. These studies include measurements of capture-ionization [6,7], capture-excitation [8], double capture [9], and double excitation [10].

The availability of heavy, highly charged ions in a large energy domain opens new possibilities for multiple process investigations in few-electron ions, beyond the helium atoms. One of such opportunity is the study of the simultaneous ionization and excitation in helium-like heavy ions in single collisions with neutral target atoms. The virtue of investigating the process of simultaneous excitation and ionization is that one electron ends up in the continuum, while the other electron ends up in a hydrogen-like final state. Due to this the two-electron process can be in principle treated as a single-electron process.

Experimentally, the identification of excitation-ionization events is greatly facilitated in the case of He-like ions where electron capture cannot lead to ground-state x-ray emission due to the initially occupied K shell. It is important to mention here that the single-collision conditions can be uniquely studied at the internal gas-jet target where gas densities of about 10^{12} particles/cm^3 [11] are provided. This can be compared with a typical density of a solid-state target of about 10^{21} particles/cm^3. Using solid targets [2,12,13], a measurement of two-electron processes is more difficult due to the high probabilities of excitation and ionization occurring in two successive collisions. In contrast, for gas targets the probability for a two-step excitation and ionization process is negligible. The cross section of this process can be determined
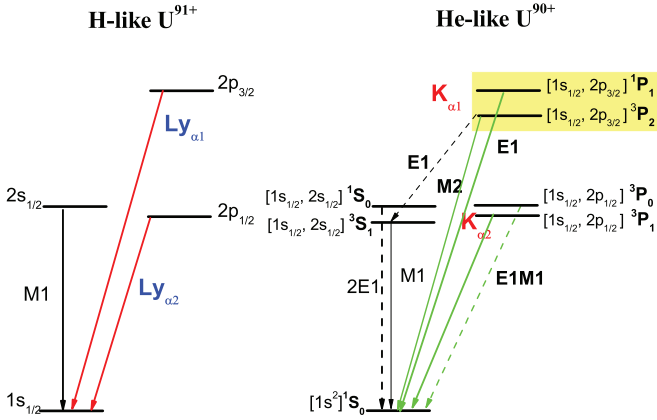
*S.Salem@gsi.de

FIG. 1. (Color online) Level diagram of the first excited levels in H- and He-like U. Multipolarities for the most probable decay modes are indicated by solid arrows; weaker decay modes are shown as dashed arrows.

directly from the Ly$_\alpha$ radiation measured in coincidence with the projectile having lost one electron.

In this paper, we report on the single-electron processes for high-Z projectiles at relativistic collision velocities ($\beta = v_{\text{proj}}/c \simeq 0.60$, where v_{proj} is the projectile velocity and c is the speed of light). The main goal of the present investigation was to extend the information on the population of the excited states of H- and He-like uranium ions (see Fig. 1) and, in addition, the possibility to investigate the impact parameter characteristics of two different processes, namely the process of simultaneous excitation and ionization and the single-excitation process.

The paper is structured as follows: In Sec. II, a brief overview of the theoretical methods used for the description of simultaneous excitation and ionization processes will be outlined. The experimental arrangement used for the measurement and the measured x-ray spectra will be described in Sec. III. In Sec. IV, the experimental results are presented and explained on the basis of the semiclassical approximation for the projectile ionization and excitation and by assuming the independent-particle model. Finally, in Sec. V, a short summary is given.

II. BACKGROUND

The theoretical description of excitation and ionization in helium-like systems relies on two assumptions. First, the process is described within the framework of the independent-particle approximation (IPA), in which the electrons are assumed to move independently of each other in the average field generated by the nucleus and the other electrons. Therefore in this approximation, the processes of the excitation and ionization are not correlated. Second, the single-electron processes are described in the assumptions of the classical trajectory model of the internuclear motion.

For a classical description of atomic collisions, it is useful to introduce the concept of the impact parameter. It is assumed that, during the collision, the particle follows a classical trajectory with an incoming and an outgoing branch. The asymptote to the incoming branch is parallel to the beam direction while the asymptote to the outgoing branch defines the deflection angle θ with respect to the incoming beam
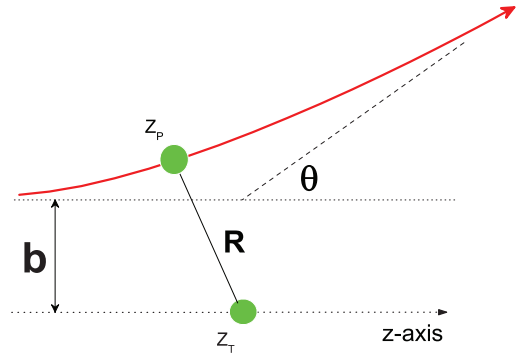

FIG. 2. (Color online) The classical trajectory of a particle in the laboratory system, defined by the impact parameter **b** and the scattering angle θ.

direction. The distance from the scattering center to the projectile is denoted as the impact parameter **b**, where the bold notations denote vectorial quantities (see Fig. 2).

A. Excitation and ionization probability

For the calculation of the transition probabilities and of the cross section for excitation of high-Z projectile ions, at relativistic velocities, a complete Liénard-Wiechert interaction potential must be considered [14]. To calculate the cross section between any pair of specified initial and final states, i and f, the impact parameter dependent transition probability can be expressed in terms of the transition amplitude A_{fi}:

$$P_{fi}(b) = |A_{fi}|^2. \tag{1}$$

The transition amplitude for excitation of a projectile electron can be written as [15]

$$A_{fi}(b) = i\gamma Z_P e^2 \int dt\, e^{i(E_f - E_i)t} \int d^3r\, \psi_f^\dagger(\mathbf{r}) \frac{1 - \beta\hat{\alpha}_z}{r'} \psi_i(\mathbf{r}), \tag{2}$$

where $\gamma = (1 - \beta^2)^{-1/2}$, $\beta = v/c$, and $\hat{\alpha}_z$ is the Dirac matrix in the z direction. r' is the electron-projectile distance measured in the projectile system. E_i, ψ_i and E_f, ψ_f are the initial and final energies and wave functions of the electron, respectively.

For the description of the impact parameter dependent ionization, a semiclassical approximation (SCA) originally developed by Bang and Hansteen [16] is adopted. In the SCA, the ionization probability $P^{\text{ion}}(b)$ is determined within first-order perturbation theory. Based on the SCA, Trautmann and Rösel developed a model to calculate the ionization cross section [17]. The model neglects the magnetic part of the full interaction potential, and assumes nonrelativistic collision kinematics. However, exact Dirac wave functions are used.

The magnetic contribution to the total ionization amplitude arises if one considers a relativistic collision where the perturbing spherically symmetrical Coulomb potential is Lorentz transformed to the laboratory frame of the ionized atom. This transformation leads to the extension of the potential in the transverse direction and shrinkage in the longitudinal direction, yielding the Liénard-Wiechert potential [14]. Within this picture, the magnetic part of the interaction amplitude is added incoherently. This correction leads to an increase of

the total ionization cross sections with increasing β values. It should be noted that the model proposed by Anholt *et al.* [18], where electric and magnetic contributions are added incoherently, generally yields a fairly good agreement with the existing experimental cross section data [19,20], with one interesting exception at ultrarelativistic energies [21].

B. The simultaneous excitation and ionization

The consequence of the independent-particle approximation is that the many-body problem can be reduced to a single-electron problem. In this approach the probability for a simultaneous ionization and excitation of the ground-state electrons into the final nlj state of the projectile, $P_{nlj}^{\text{ion-exc}}$, can be expressed as an uncorrelated product of single-electron probabilities:

$$P_{nlj}^{\text{ion-exc}}(b) \approx P^{\text{ion}}(b) P_{nlj}^{\text{exc}}(b). \qquad (3)$$

Here, $P^{\text{ion}}(b)$ is the single-electron ionization probability for collision with an impact parameter **b** and P_{nlj}^{exc} is the single-electron excitation probability into the state characterized by quantum numbers nlj. The total cross section for the process of ionization and excitation into the nlj state of the projectile is then given by

$$\sigma_{nlj}^{\text{ion-exc}} = \int_0^\infty 2\pi b\, P_{nlj}^{\text{ion-exc}}(b)\, db. \qquad (4)$$

Using Eqs. (3) and (4), the cross section for the simultaneous ionization and excitation processes can be derived.

C. Calculated probabilities in the independent-particle model

The curves representing calculated probabilities of individual single-electron processes for a 220 MeV/uU^{91+} projectile are shown in Fig. 3(a). In the case of excitation, only probabilities for the population of the $2s_{1/2}$, $2p_{1/2}$, and $2p_{3/2}$ states summed over the final magnetic substates are presented. The probability for K-shell ionization of U^{91+} calculated within the SCA approximation is also shown. One can observe that the excitation probability into the $2s_{1/2}$ state reaches its maximum at much smaller impact parameters than that for the $2p$ states. According to Eq. (3), the reduced probabilities for the simultaneous excitation and ionization process in He-like uranium ions are plotted in Fig. 3(b). Due to its multiplicative nature, the impact parameter dependence of excitation plus ionization exhibits a prominent suppression of probabilities at large impact parameters as compared to the single-electron processes. Hence, the cross sections for the simultaneous excitation plus ionization can be regarded as equivalent to the impact parameter differential measurement in the sense that they probe the individual single-electron processes at small impact parameter b. The calculated cross section ratios $\frac{\sigma^{\text{exc}}(\text{Ly}_{\alpha 1})}{\sigma^{\text{exc}}(\text{Ly}_{\alpha 2})}$ are considerably different for single excitation and excitation accompanied by K-shell ionization, and are equal to 0.84 and 0.42 [22], respectively.

D. Alignment of the excited-ion states

One has the possibility to study the population mechanism on the magnetic subshell in few-electron highly charged heavy ions (see Fig. 1). Information on the population of magnetic
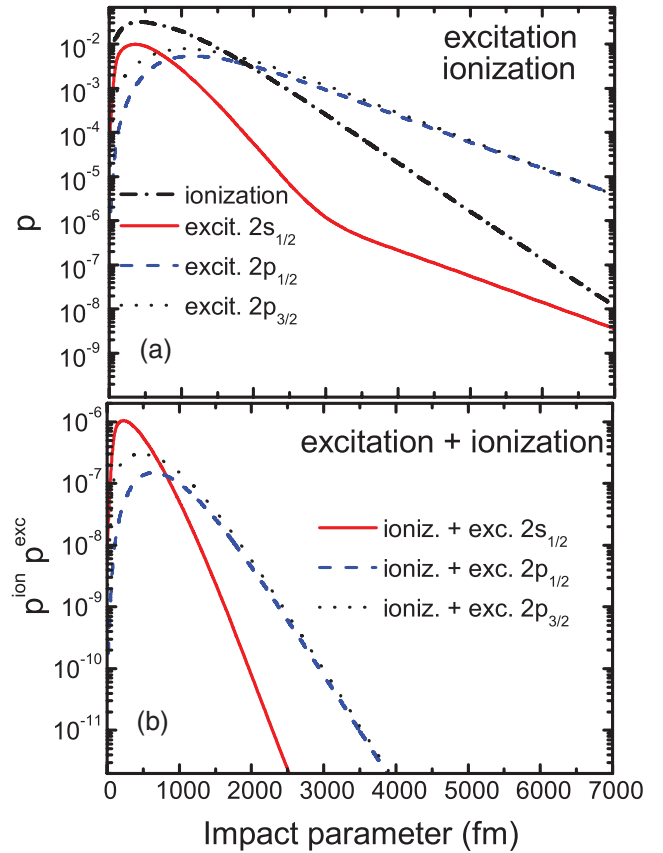

FIG. 3. (Color online) Calculated probabilities for excitation and ionization in hydrogen-like uranium ions and excitation-ionization processes helium-like uranium ions, plotted versus collision impact parameter [22].

substates can be obtained by the study of angular distributions of the emitted photons. The angular distribution of the photons in the emitter frame is related to the alignment parameter by [23,24]

$$W(\theta) = A_0 + A_2 P_2(\cos\theta') \propto 1 + \beta_{20}\left(1 - \tfrac{3}{2}\sin^2\theta'\right), \qquad (5)$$

where θ' is the angle between the direction of the deexcitation photon and the beam direction while $P_2(\cos\theta')$ denotes the second-order Legendre polynomial. The well-known expression (6) takes into account only the dominant electric dipole (E_1) term whereas the weaker magnetic quadrupole decay (M_2) is neglected. As seen from Eq. (6), the angular distribution is determined by the so-called *anisotropy* coefficient $\beta_{20} = \alpha A_{20}$, while the coefficient α depends only on the total angular momenta of the initial and final ionic states, respectively. For the case of the $2p_{3/2} \rightarrow 1s_{1/2}$ transition, $\alpha = 1/2$ [23].

The population of magnetic sublevels is likely to deviate from a statistical distribution. In such cases the levels are aligned; thereby the pairs of atomic sublevels with the same magnetic quantum number (but with opposite signs) will be necessary equally populated. Here, it is assumed that neither the ions nor the the target atoms are polarized in ion-atom collisions. Consequently, the state of the ion is axially symmetric about z. This restricts the anisotropy parameters $A_{k\kappa}(\kappa = -k + \cdots + k)$ of the state to A_{k0}, where k can take

only even values $2, 4, \ldots, 2J - 1$. It follows that only states with $J \geqslant 3/2$ are aligned. The alignment of an atomic level is commonly described in terms of one or several parameters A_{kk} which are related to the the population cross sections $\sigma(\mu_n)$ of the various sublevels μ_n. For example, for $J = 3/2$ the alignment parameter can be expressed as [23]

$$A_{20} = \frac{\sigma\left(\frac{3}{2}, \pm\frac{3}{2}\right) - \sigma\left(\frac{3}{2}, \pm\frac{1}{2}\right)}{\sigma\left(\frac{3}{2}, \pm\frac{3}{2}\right) + \sigma\left(\frac{3}{2}, \pm\frac{1}{2}\right)}, \qquad (6)$$

where $\sigma(2p_{3/2}, \mu_n)$ describes the population of substate μ_n of the $2p_{3/2}$ level.

III. EXPERIMENT

A. Experimental arrangement

The measurement of the simultaneous excitation and ionization processes was carried out using the internal gas-jet target of the experimental storage ring ESR at GSI. He-like uranium ions with an incident energy of 220 MeV/u were selected and guided towards the ESR. In the ESR, the ions were cooled and stored for quite long times. After the cooling, the relative momentum spread of the injected ion beam is reduced from $\Delta p/p \approx 10^{-3}$ to about 10^{-5}. After completion of the cooling cycle, the gas-jet device was switched on. A molecular xenon gas-jet target with typical densities $\sim 10^{12}$ particles/cm^3 was used.

The x rays emitted from the ion-atom collisions were recorded by high-purity germanium detectors placed at different observation angles. The accessible angles are $35°$, $60°$, $90°$, $120°$, and $150°$ with respect to the beam direction. The different germanium detectors were isolated from the ultrahigh vacuum environment by 50 μm stainless steel or 100 μm thick beryllium windows. Having different crystals, the energy resolution and the detection efficiency is different from one detector to the other. This is reflected in the quality of the registered x-ray spectra. To get the best possible energy separation of the lines of interest in the x-ray spectra, the Doppler broadening was reduced by using collimators with different solid angles. The collimators were made of lead having different slit thicknesses and widths. In general, these collimators defined the solid angle of the individual detectors located at $35°$, $60°$, $90°$, $120°$, and $150°$, to about 1.08×10^{-4}, 6.77×10^{-5}, 3.18×10^{-5}, 2.39×10^{-5}, and 1.94×10^{-4} sr, respectively. For more details, see Ref. [25]. A sketch of the experimental arrangement at the present interaction chamber of the ESR gas-jet is shown in Fig. 4.

After passing through the target region, the projectiles that lost ($Q = 91+$) or captured ($Q = 89+$) one electron were separated from the primary beam behind the next dipole magnet of the ring. For the study of ionization and capture processes, both the up-charged (H-like) and down-charged (Li-like) uranium ions were registered by two dedicated *multiwire proportional counters* (MWPC) placed on the internal and external side of the ring. The detection efficiency of the ions is better than 99% [26].

The detector signals are processed using standard NIM electronics. Hardware coincidence between the germanium and particle detectors is used. For the data acquisition, it is based on the multibranch system (MBS) developed at GSI.
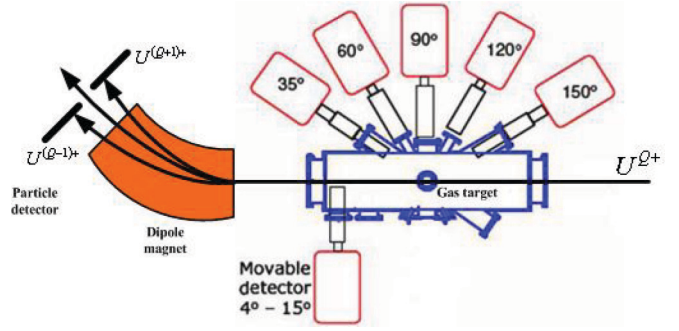

FIG. 4. (Color online) Layout of the experimental arrangement at the ESR jet target. Photon emission is observed in coincidence with the up- or down-charged ions, detected by a particle counter placed behind the dipole magnets.

The MBS runs under the operating system Lynx on a CAMAC processor board CVC. The system works stand alone; it reads all data from the CAMAC modules and writes them on a local tape drive or directed on the disk.

B. X-ray spectra

Figure 5 shows an x-ray spectrum recorded for initially He-like uranium ions colliding with xenon target atoms at the energy of 220 MeV/u. The spectrum was recorded by using the germanium detector located at $35°$ in coincidence with the up-charged (U^{91+}) ions. In this spectrum, two groups of lines have been identified. In the low-energy region, the strong Xe-transition lines are visible. The presence of these lines is due to the ionization of the Xe target by the projectile during the collisions. In the high-energy part of the spectrum four different transition lines belonging to the uranium projectile are present. These transition lines give information about the different collision processes leading to the projectile x-ray emission.

In order to disentangle the contributions from the different collision processes, the coincidence time spectrum was used. Only the true coincidence between photons and up-charged H-like uranium ions are selected. To reduce the background
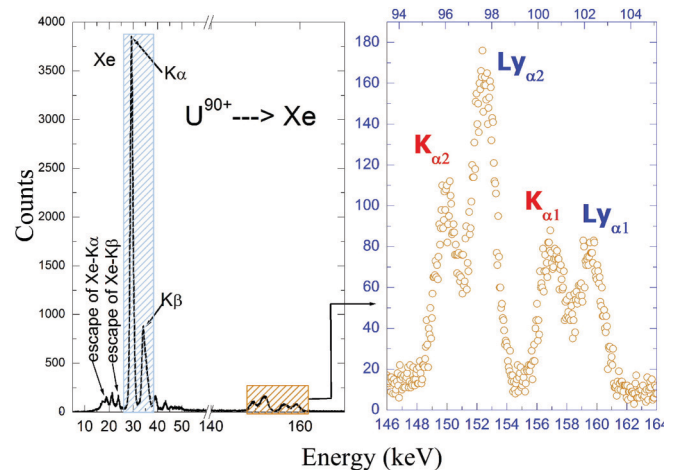

FIG. 5. (Color online) X-ray energy spectrum as observed by the germanium detector at $35°$.
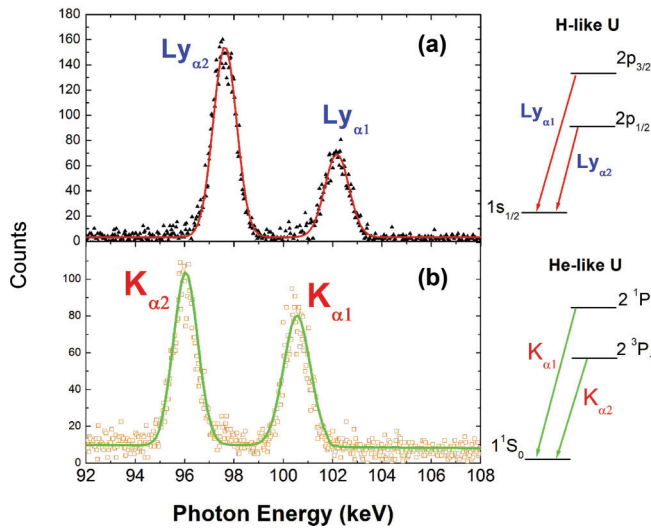
FIG. 6. (Color online) The x-ray energy spectra, recorded at $35°$, for the collision of initially He-like uranium ions with xenon target at 220 MeV/u. The K_α transitions are connected to the projectile excitation and the Ly_α lines were recorded in coincidence with the H-like uranium ions.

photons and produce a clean ground-state x-ray energy spectrum, different possibilities in the data analysis have been used, applying the condition on the coincidence spectrum to produce a new energy spectrum and vice versa. Using this technique, the background photons in the x-ray spectra disappear and a clean spectrum is produced. The clean energy spectrum corresponding to the coincidence with the H-like uranium ions is shown in Fig. 6(a).

In order to distinguish the difference between the process of excitation-ionization and the excitation process, the spectrum represented in Fig. 6(a) was subtracted from that in Fig. 5. The result of this technique is shown in Fig. 6(b). After the disentanglement, the energy spectra were corrected for the Doppler shift and the detection efficiency. In addition, the separated spectra were fitted using a Gaussian-amplitude function.

As seen in Fig. 6, the emission lines ($Ly_{\alpha1}$, $Ly_{\alpha2}$, $K_{\alpha1}$, and $K_{\alpha2}$) are well resolved and visible. A strong change in the relative intensities of the $Ly_{\alpha1}$ and $Ly_{\alpha2}$ components can be noticed. This feature reveals the energy dependence of the population of the excited projectile levels. In other words, the $Ly_{\alpha2}$ is not only the electric dipole transition (E_1: $2p_{1/2} \to 1s_{1/2}$) to be the dominant one but also the magnetic transition (M_1: $2s_{1/2} \to 1s_{1/2}$) is considered. This striking feature confirms the fact that the relativistic effects are manifested by the strongly enhanced importance of the magnetic transitions.

Also, it is interesting to note the significant change in the relative intensities of the $Ly_{\alpha1}$ and $Ly_{\alpha2}$ lines with respect to the $K_{\alpha1}$ and $K_{\alpha2}$ lines. For the case of single excitation, the experimental ratio $K_{\alpha1}/K_{\alpha2} = 0.85 \pm 0.02$, while for the simultaneous excitation and ionization process, the experimental ratio $Ly_{\alpha1}/Ly_{\alpha2} = 0.45 \pm 0.03$. This difference is due to the population mechanisms of the excited states in H- and He-like uranium ions. For completeness, to cover the study of the angular distributions for the simultaneous ionization

and excitation process, the spectra recorded by the detectors located at all different observation angles were analyzed in a similar way.

IV. RESULTS AND DISCUSSION

As discussed in detail in Ref. [27] the $Ly_{\alpha2}$ transition, arising from the decay of the ($2p_{1/2} \to 2s_{1/2}$), shows an isotropic emission pattern. Consequently, it provides an ideal tool to measure a possible anisotropy of the $Ly_{\alpha1}$ and K_α transitions. For the collisions of the initially He-like uranium ions with xenon gas-target at 220 MeV/u, the angular distribution of the $Ly_{\alpha1}$, $K_{\alpha1}$, and $K_{\alpha2}$ transitions is shown in Fig. 7. These transitions are normalized to the $Ly_{\alpha2}$ transition. The error bars shown in Fig. 7 represent the statistical uncertainties of the measured transition lines. According to Eq. (6), the best fits of the experimental data are represented by dashed and solid lines.

As seen from Fig. 7, for the $K_{\alpha2}$ transition, no alignment is observed which is probably due to the interference between the magnetic and electric dipole (E_1M_1). In this case, the $K_{\alpha2}$ transition is assumed to be isotropic. For the $K_{\alpha1}$ transition, a value of -0.036 ± 0.015 for the alignment parameter A_{20} was obtained. This agrees well with the theoretical prediction for the alignment parameter which has a small negative value (-0.034). This indicates that almost no alignment is observed and therefore the magnetic substates are statistically populated. This means that the alignment of the different sublevels, namely $[1s_{1/2}2p_{3/2}]^1P_1$ and $[1s_{1/2}2p_{3/2}]^3P_2$, is possible.

For comparison, the angular distribution of the $Ly_{\alpha1}$ has large negative value of the alignment parameter (A_{20}) which reflects the nonstatistical population of magnetic sub-states of the $2p_{3/2}$ level. The alignment parameter deduced from the experimental data is $A_{20} = -0.201 \pm 0.03$. The experimental result agrees with the theoretical prediction of the alignment ($A_{20} = -0.337$) for the simultaneous ionization and excitation.

Using the experimental angular distribution of the $Ly_{\alpha1}$ and $K_{\alpha1}$ transitions, it is possible to investigate the impact parameter characteristics of the simultaneous ionization-excitation
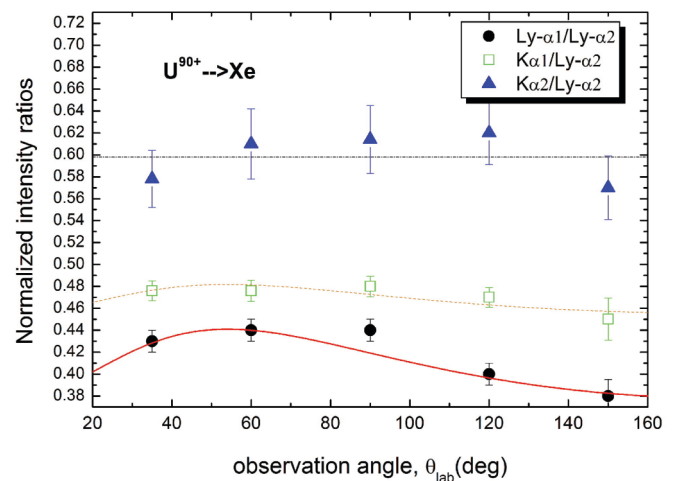

FIG. 7. (Color online) The intensities of $K_{\alpha2}$ (up-triangles), $K_{\alpha1}$ (open squares), and $Ly_{\alpha1}$ (solid circles) normalized to the $Ly_{\alpha2}$ line as a function of the observation angles.
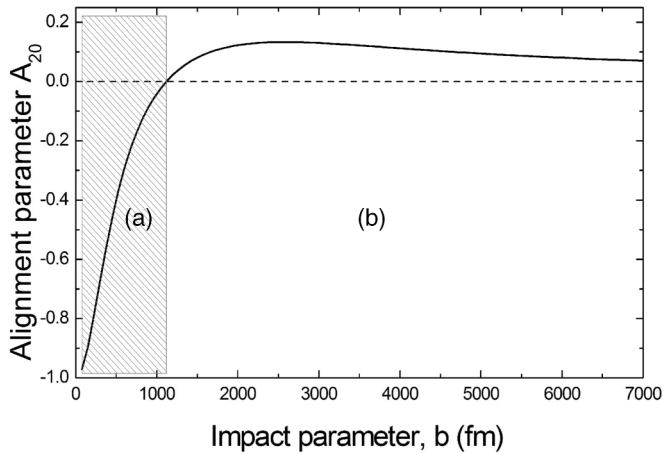
FIG. 8. Degree of alignment parameter versus impact parameter for the $2p_{3/2}$ state [22]. The difference of the impact parameter dependence between (a) the simultaneous ionization and excitation and (b) the single-electron processes.

and the single-electron excitation processes, respectively. The dependence of the alignment parameter on the collision impact parameter, as calculated in Ref. [22], is shown in Fig. 8. From the dependence of the alignment parameter A_{20} on the collision impact parameter b, it is possible to estimate the impact parameter range for the simultaneous ionization and excitation process ($b^{\text{ion-exc}} = 810$ fm). There is a good agreement between the experiment and the theory in which the collision occurs only at small impact parameter. This allows for the conclusion that the experimental results confirm the theoretical predictions for the validity of first-order perturbation theory at relativistic energies. It is worthwhile to conclude that the anisotropic emission observed for the $\text{Ly}_{\alpha1}$

transition provides impact parameter sensitive information about the single-electron excitation.

V. SUMMARY

The present work reports on the study of a two-electron process: the simultaneous ionization and excitation occurring in relativistic collisions of heavy, highly charged ions with gaseous targets. The investigation was performed on He-like uranium ions impinging upon a xenon gas-target at an incident energy of 220 MeV/u. The measurements have been performed at the ESR gas-target using atomic xenon. To select this process, the Lyman-series (Ly_α) radiation has been measured at various observation angles in coincidence with up-charged projectiles (U^{91+}). From the yields of the $\text{Ly}_{\alpha1}$ and $\text{Ly}_{\alpha2}$ projectile radiation, the relative cross section for the process of simultaneous ionization and excitation was directly determined. The angle-dependent measurement of the radiation yields provides information about the angular distributions of the emitted radiation and permits the determination of the alignment parameter A_{20}. This parameter gives information on the level population and the collision impact parameter. The present results show that the simultaneous ionization and excitation is a process which occurs at small impact parameter.

[1] T. Stöhlker, C. Kozhuharov, P. H. Mokler, A. Warczak, F. Bosch, H. Geissel, R. Moshammer, C. Scheidenberger, J. Eichler, A. Ichihara, T. Shirai, Z. Stachura, and P. Rymuza, Phys. Rev. A **51**, 2098 (1995).

[2] T. Stöhlker, D. C. Ionescu, P. Rymuza, F. Bosch, H. Geissel, C. Kozhuharov, T. Ludziewjewski, P. H. Mokler, C. Scheidenberger, Z. Stachura, A. Warczak, and R. W. Dunford, Phys. Rev. A **57**, 845 (1998).

[3] J. H. McGuire, Phys. Rev. A **36**, 1114 (1987).

[4] J. H. McGuire, Adv. At. Mol. Opt. Phys. **29**, 217 (1992).

[5] P. A. Hayes and J. F. Williams, Phys. Rev. Lett. **77**, 3098 (1996).

[6] D. Vernhet, L. Adoui, J. P. Rozet, K. Wohrer, A. Chetioui, A. Cassimi, J. P. Grandin, J. M. Ramillon, M. Cornille, and C. Stephan, Phys. Rev. Lett. **79**, 3625 (1997).

[7] L. H. Andersen, M. Frost, P. Hvelplund, H. Knudsen, and S. Datz, Phys. Rev. Lett. **52**, 518 (1984).

[8] J. A. Tanis, E. M. Bernstein, M. W. Clark, W. G. Graham, R. H. McFarland, T. J. Morgan, B. M. Johnson, K. W. Jones, and M. Meron, Phys. Rev. A **31**, 4040 (1985).

[9] N. Stolterfoht, C. C. Havener, R. A. Phaneuf, J. K. Swenson, S. M. Shafroth, and F. W. Meyer, Phys. Rev. Lett. **57**, 74 (1986).

[10] J. O. P. Pedersen and P. Hvelplund, Phys. Rev. Lett. **62**, 2373 (1989).

[11] J. Eichler and T. Stöhlker, Phys. Rep. **439**, 1 (2007).

[12] S. Salem, A. Bräuning-Demian, R. Dunford, F. Bosch, H. Bräuning, S. Chatterjee, S. Hagmann, C. Kozhuharov, D. Liesen, P. H. Mokler, Z. Stachura, and A. Warczack, GSI Report 2006-1 (2006).

[13] T. Ludziejewski, T. Stöhlker, H. Beyer, F. Bosch, S. Fritzsche, D. C. Ionescu, C. Kozhuharov, A. Krämer, D. Liesen, P. H. M. P. Rymuza, Z. Stachura, P. Swiat, and A. Warczak, Nucl. Instrum. Methods Phys. Res., Sect. B **154**, 204 (1999).

[14] J. Eichler and W. E. Meyerhof, *Lectures on Ion-Atom Collisions: From Nonrelativistic to Relativistic Velocities* (Elsevier, Amsterdam, 2005).

[15] J. Eichler and W. E. Meyerhof, *Relativistic Atomic Collisions* (Academic Press, San Diego, 1995).

[16] J. M. Hansteen, O. M. Johnson, and L. Kocbach, At. Data Nucl. Data Tables **15**, 305 (1975).

[17] D. Trautmann and F. Rösel, Nucl. Instrum. Methods **169**, 259 (1980).

[18] R. Anholt, Phys. Rev. A **19**, 1004 (1979).

[19] R. Anholt, Phys. Rev. A **31**, 3579 (1985).

[20] T. Stöhlker, D. C. Ionescu, P. Rymuza, T. Ludziejewski, P. H. Mokler, C. Scheidenberger, F. Bosch, H. Geissel, O. Klepper, C. Kozhuharov, R. Moshammer, F. Nickel, H. Reich, Z. Stachura, and A. Warczack, Nucl. Instrum. Phys. Res. B **124**, 160 (1997).

[21] H. F. Krause, C. R. Vane, S. Datz, P. Grafström, H. Knudsen, C. Scheidenberger, and R. H. Schuch, Phys. Rev. Lett. **80**, 1190 (1998).

[22] T. Ludziejewski, T. Stöhlker, D. C. Ionescu, P. Rymuza, H. Beyer, F. Bosch, C. Kozhuharov, A. Krämer, D. Liesen, P. H. Mokler, Z. Stachura, P. Swiat, A. Warczak, and R. W. Dunford, Phys. Rev. A **61**, 052706 (2000).

[23] E. G. Berezhko and N. M. Kabachnik, J. Phys. B: At. Mol. Phys. **10**, 2467 (1977).

[24] J. Eichler, A. Ichihara, and T. Shirai, Phys. Rev. A **58**, 2128 (1998).

[25] S. Salem, Ph.D. thesis, Frankfurt University, Institut für Kernphysik-Frankfurt, 2010.

[26] O. Klepper and C. Kozhuharov, Nucl. Instrum. Methods Phys. Res., Sect. B **204**, 553 (2003).

[27] T. Stöhlker, F. Bosch, A. Gallus, C. Kozhuharov, G. Menzel, P. H. Mokler, H. T. Prinz, J. Eichler, A. Ichihara, T. Shirai, R. W. Dunford, T. Ludziejewski, P. Rymuza, Z. Stachura, P. Swiat, and A. Warczak, Phys. Rev. Lett. **79**, 3270 (1997).